RESEARCH

The vibration propagation and damage distribution characteristics of deep-buried underground cavern blasting

Junlin Lv[1] · Zhen Liu[1] · Junhong Huang[2]

Abstract

With the increase of the scale of an underground cavern, more and more towering underground side walls are left behind by blasting operation, which leaves a huge hidden danger to the structure safety of an underground cavern. Taking the propagation mechanism and damage distribution characteristics of blasting vibration along the elevation direction as the research subject, the propagation mechanism of blasting vibration along the elevation direction of high side wall of a deep-buried underground cavern can be obtained by comprehensive application of theoretical analysis, dimensional analysis, formula derivation, numerical analysis, and other research methods. Through multiangle comparative analysis, the internal mechanism of blasting vibration under elevation effect in underground caverns is revealed, and combined with the relationship between surrounding rock damage and blasting vibration velocity, the distribution characteristics of blasting vibration and damage under the elevation effect are proposed. In addition, through the establishment of a mechanical model of the response of blasting vibration of underground high side walls, the prediction formula of particle vibration velocity along the elevation direction under blasting vibration condition is analyzed, and the formula is adjusted and modified, which can meet the developing requirements of surrounding rock damage control precision.

Keywords Elevation effect · Blasting vibration · Surrounding rock damage · Distribution characteristic

1 Introduction

Various negative effects of blasting excavation are led by blasting seismic effect, it will not only affect the surrounding buildings and environment, but also seriously affect the durabil-

✉ J. Lv
JLLv_sdtbu@163.com

1   School of Management Science and Engineering, Shandong Technology and Business University, Yantai, 264005, Shandong, China

2   School of Resources and Environmental Engineering, Wuhan University of Technology, Wuhan, 430070, Hubei, China

ⵁ Springer

ity and safety of the whole project. In fact, there is a certain relationship between blasting seismic effect and blasting vibration propagation and attenuation (Cai et al. 2004). Delun Wu proposed as follows (Wu and Ye 2004): When judging the blasting vibration safety of underground workshop, critical vibration velocity should be calculated and predicted according to different frequency segments. Tang et al. (2001) found the qualitative relationship between main vibration frequency and ground particle blasting vibration velocity. Li et al. (2006) made a comprehensive and in-depth study on the actual data of blasting vibration velocity by using the qualitative and quantitative analysis method and found that there are significant differences in the response of various structures to blasting vibration. Shi and Bi (2004) completed the division of seismic wave signals according to each frequency band through Fourier transform and other research methods and studied the frequency attenuation law of seismic waves by taking frequency as the standard. Zhou et al. (2011) introduced a dimensional analysis method to deduce and simulate the formula of blasting vibration attenuation rule under the condition of spherical cavity, and then carried out fitting analysis through measured data and numerical simulation and verified the reliability and effectiveness of the above attenuation formula.

During blasting excavation, explosion load will burst out huge energy and destroy the rock mass structure, but in this process, it will also cause damage to the rock mass retained. In view of this phenomenon, domestic and foreign scholars through a large number of experimental studies explored and analyzed the dynamic load induced damage mechanism of surrounding rock (Yang et al. 2018; Zhao et al. 2011). Grady and Kipp (1980) pointed out that there are original fractures in the original rock that will be activated and continue to coalesce and expand when subjected to large external forces, resulting in rock failure. Tylor et al. (1986) selected mechanical parameters such as Poisson's ratio, elastic modulus, and crack density, analyzed the relationship between them and the damage coefficient, and created the damage model on this basis. Kuszmaul (1987) summarized the previous research results, discussed the damage mechanism of rock mass from two perspectives of compression and tensile, and built the KUS damage model. Thorne et al. (1990) took different damage variables as the precondition and used KUS damage model to explore the relationship between crack activation number, rock mass volume, and damage coefficient. Yang et al. (1996) modified the KUS model based on his own research needs and further pointed out that only when the strain stress reaches a certain critical value, crack propagation of rock mass materials will be activated, resulting in damage to rock mass.

According to the analysis of previous research results, it is found that the research objects of the elevation effect of blasting vibration are often concentrated in open-pit slope and high-rise buildings, and there are few research works on the elevation effect of blasting vibration of an underground cavern. At the same time, many scholars have established mechanical models and constitutive models for surrounding rock damage characteristics, but the relation between blasting vibration distribution mechanism and surrounding rock damage characteristics is rarely proposed. In this paper, the method of combining field test and numerical simulation is used to interpret and describe the blasting vibration propagation law and surrounding rock damage distribution characteristics of deep underground caverns in a more comprehensive way, and at the same time to provide certain theoretical basis and guidance for the protection and influence control of blasting vibration construction of high side walls of large and complex underground caverns.

2 Theoretical study on the blasting vibration propagation law of a high side wall of an underground cavern

2.1 Theoretical formula of the blasting vibration propagation law of a high side wall

Based on many experiments, Sadowski proposed a widely used formula for predicting vibration velocity, as shown below (Huang et al. 2020):

$$V = K\left(\frac{\sqrt[3]{Q}}{R}\right)^{\alpha}. \tag{1}$$

Through the accumulation of many engineering practices, Zhu et al. (1988) finally realized that the formula proposed by Sadowski did not reflect how elevation factors affected blasting vibration, so the improved formula was subsequently proposed:

$$V = K\left(\frac{\sqrt[3]{Q}}{R}\right)^{\alpha}\left(\frac{\sqrt[3]{Q}}{H}\right)^{\beta}. \tag{2}$$

H is the elevation difference between the measuring point and the source of detonation, and m is taken as the unit. It is equivalent to the parameters of formula (1).

Zhou et al. (1997), after analyzing many measured data of blasting vibration, summarized the approximate formula that could reflect the elevation effect:

$$V = K\left(\frac{\sqrt[3]{Q}}{R}\right)^{\alpha} H^{u}. \tag{3}$$

The value of u is related to the height difference. The value of u is selected according to the hardness of rock. The higher the hardness, the higher the value.

Song et al. (2000) adopted the field blasting vibration test method to test the slope of an open-pit iron mine. After analyzing the measured data, the following blasting vibration formula is formed considering the influence of height difference:

$$V = K\left(\frac{\sqrt[3]{Q}}{R}\right)^{\alpha}\left(\frac{R}{S}\right)^{\beta}. \tag{4}$$

In the formula, R/S, the basic coefficient of influence of height difference, can be combined with the ratio of the oblique distance and horizontal distance corresponding to the detonation center and the measuring point.

Xu et al. (2007) clearly pointed out in his research report that Sadowski's formula did not take into account the influence of blasting free surface conditions, which affected the accuracy and reliability of blasting vibration velocity measurement to a certain extent. In view of this defect, the scholar pointed out that the influence degree of free surface area on blasting vibration could be included in the category of calculation, and on this basis, Sadowski's revised formula was proposed:

$$V = K\left(\frac{\sqrt[3]{Q}}{R}\right)^{\alpha} (A)^{\beta}. \tag{5}$$

In the above expression, the parameters A and β represent the area parameter and the area index of the free surface of section blasting, respectively.

When the propagation law of particle vibration velocity affected by elevation difference of observation points is taken into account, the attenuation law of wave velocity can be measured and predicted by combining the following formula. In this case, the significance of some parameters should be changed, that is, the detonation distance should be set as horizontal distance. The other parameters remain the same (DL/T 5389-2007).

$$V = K \left(\frac{\sqrt[3]{Q}}{D} \right)^{\alpha} \left(\frac{\sqrt[3]{Q}}{H} \right)^{\beta}. \tag{6}$$

2.2 Mechanical model analysis of a high side wall of an underground cavern based on simply supported beam characteristics

Compared with semiinfinite space, the propagation of natural earthquakes is affected by the "cavity effect" and "terrain effect" of underground caverns, that is, the vibration wave will produce complex reflection and diffraction on the surface of surrounding rock of caverns. For the blasting excavation of the interior part of the tunnel, the vibration response of the side wall under the excitation of blasting load is more considered (Zhang et al. 2018; Ramulu et al. 2009). Different from open-air high-rise buildings and rock-soil slopes, which are usually simplified into cantilever beam models, the upper and lower ends of the surface surrounding rock of the underground cavern side wall are constrained by the roof and floor, which have typical characteristics of simple supported beams, but are different from ordinary simple supported beams. This paper uses simplified conditions to analyze, as is shown in Fig. 1.

When considering the vibration of high-rise buildings caused by ground vibration, modal analysis is often used to determine the vibration response modes at different frequencies (Pei et al. 2006). A simplified structural mechanics analysis model and the dynamic analysis method for rock and soil mass have been investigated (Liu et al. 2007; Terzaghi 1955; Liu 2004). With extensive reference to the simplified mechanical analysis model of retaining wall, vertical slope, and elastic foundation beam, as well as the simple algorithm (Zheng et al. 2005) provided by Japan's seismic criterion for chemical equipment, the surrounding rock continuum is abstracted as multiple rock layers, the surface surrounding rock of a side wall is abstracted as beam, and the elastic connection between deep and surface surrounding rock is set (as shown in Fig. 1). A rotating spring is used to simplify the constraint condition of the beam end. When analyzing a section of an underground cavern, one side wall is simplified into a simply supported beam due to the constraints of both upper and lower ends. The load it receives can be equivalent to the axial load and the transverse load, among which the axial load changes with time and the transverse load changes with location and time. The total height of the cavern is equivalent to the total length of the beam which is represented by L.

To simplify the analysis and obtain the amplification factor, which is convenient for application, this paper simplifies the constraint conditions of the end and lateral force of the surface surrounding rock, and then the differential equation of flexural vibration of the simply supported beam is as follows:

$$EI \frac{\partial^4 Y}{\partial H^4} + \overline{m} \frac{\partial^2 Y}{\partial t^2} + f(t) \frac{\partial^2 Y}{\partial H^2} = q(H) \sin(pt). \tag{7}$$

In the above equation, EI is the bending stiffness of the beam, $\overline{m}$ is the mass per unit length of the beam, and Y is the displacement function, $f(t)$ represents the harmonic excita-

(a) Analysis profile of underground cavern   (b) Mechanical model   (c) Principal mode
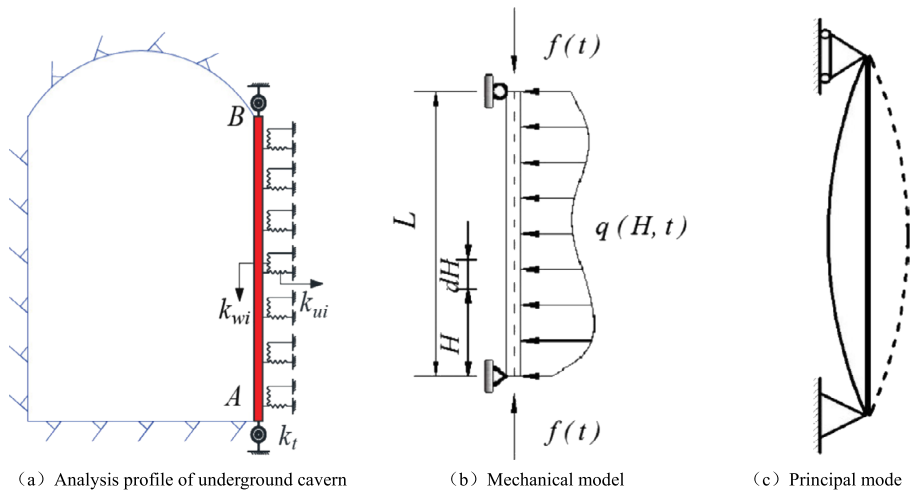
Fig. 1 Simplified calculation model of the side wall of an underground cavern

tion concentrated load acting on both ends of simple supported beam, and $q(H)$ represents the amplitude function of the interference force.

The initial condition of beam vibration is

$$\begin{cases} Y(H,0) = 0, \\ Y'(H,0) = 0. \end{cases} \tag{8}$$

The boundary conditions of beam vibration are

$$\begin{cases} Y(0,t) = Y(L,t) = 0, \\ Y''(0,t) = Y''(L,t) = 0. \end{cases} \tag{9}$$

The displacement equation of equation (9) can be solved in the following form:

$$Y(H,t) = \sum_{i=1}^{n} C_n(t) \sin \frac{n\pi H}{L}. \tag{10}$$

Partial differentiation of the above equation with respect to time, which is represented by t, yields the vibration velocity at any position at any time.

$$\frac{\partial Y(H,t)}{\partial t} = \sum_{i=1}^{n} C'_n(t) \sin \frac{n\pi H}{L}. \tag{11}$$

For the structure of rock and soil with high stiffness such as a high slope and an underground cavern, only the first order mode of vibration is considered. Therefore, the value of n in formula (10) is equal to 1, where $C_n(t)$ represents the amplitude function. Partial differentiation of the two ends of formula (10) with respect to time t is obtained to obtain the vibration velocity at any elevation position and at any time, expressed by $\frac{\partial Y(H,t)}{\partial t}$. And

Fig. 2 Field diagram of underground cavern

then the first derivative of $C_n(t)$ is calculated, expressed by $C'_n(t)$, which is the maximum velocity peak on the simple supported beam (as shown in formula (11)). Therefore, the ratio of particle vibration velocity at any point on the beam to the peak value of the maximum velocity on the beam is $\sin(\pi H/L)$. It can be used as a dimensionless quantity to characterize the ratio between the particle vibration velocity of arbitrary measuring point and the maximum velocity peak of the whole side wall.

3 Field test of blasting vibration and damage

3.1 Project overview of site test site selection

Considering the danger of blasting operation, the laboratory cannot meet the test conditions, and the use of other means to replace the blasting process has its particularity. At the same time, according to the propagation law and attenuation characteristics of blasting vibration, the blasting vibration attenuation is very rapid in the near area, the test model of general size cannot capture the elevation propagation law of blasting vibration and cannot meet the test requirements (Yang et al. 2018). Therefore, in-situ blasting vibration test is carried out in the underground cavern of Taohuazui mining area of Hubei Sanxin Gold and Copper Co., LTD., to study the law of blasting vibration propagation along the high side wall in the underground caviar. The underground cavern is 32.3 m long, 10 m wide, 12 m high, and 3876 m^3 in volume, as shown in Fig. 2.

3.2 Field measurement of blasting vibration

3.2.1 Test system and test point layout

(1) Test system

In this study, the blasting vibration wave measurement instruments mainly include: L20 vibration recorder, three-component vibration speed sensor, and client three categories. The performance of the selected instrument is good, can measure the vibration waves in three different directions at the same time, the test speed is basically maintained in 0.001 $\sim$ 35.5 cm/s, the test frequency range is controlled in 1 $\sim$ 1000 Hz, the test accuracy is 5%, the reading accuracy of the instrument is 0.1%.

(2) Measuring point layout

To obtain the propagation law of blasting vibration in the elevation direction of underground caverns, blasting is carried out at the lower part of underground caverns 1 m away from the floor. Eight measuring points are arranged on the side wall of underground caverns in each test, marked as MP1 $\sim$ MP8, and the vibration velocity sensors of each measuring point are ensured to be arranged on the same vertical measuring line, which extends upward along the elevation direction. The propagation law of the same blasting vibration along the elevation direction of the side wall in underground caverns is obtained. To ensure the safety of instruments, the detonation center distance of the first measuring point is set to 2 m in the underground cave, and the spacing of each remaining blasting vibration tester is determined to be 1 m. The distribution of measuring points on the side wall of the underground cave is shown in Fig. 3, and the arrangement and installation of on-site instruments are shown in Fig. 4.

To explore the correlation between the propagation law of blasting vibration in the elevation direction and the blasting charge amount and horizontal distance during the construction of underground cavern blasting, the experimental research is carried out by changing the blasting charge amount and the horizontal distance from the blasting source to the measuring point on the basis of not changing the location of the measuring point in the underground cavern. Under the working condition of changing the dosage of the detonating charge, the two dosage sizes are confirmed respectively, which are 2 kg and 4 kg. Three groups of tests are conducted parallel to each dosage for comparative study. Under the test condition of changing the horizontal distance between the explosion source and the measuring point, the horizontal distance is determined to be 0 m, 10 m, and 20 m in three cases, respectively. Similarly, three groups of comparison tests are conducted in parallel for each horizontal distance test condition.

3.2.2 Analysis of test results

The in-situ test results of blasting vibration on the high side wall of underground caverns are recorded in Table 1. The maximum single dose of charge is represented by Q, the horizontal distance between the measuring point and the detonation source is represented by D, and the height difference between the measuring point and the detonation source is represented by H. Due to the large amount of data obtained in the test, in Table 1, the maximum peaks of particle vibration velocity in X, Y, and Z directions obtained by the three groups of underground chamber blasting tests are obtained respectively, and then the average values of the three groups of test results are calculated and sorted into Table 1. The data obtained
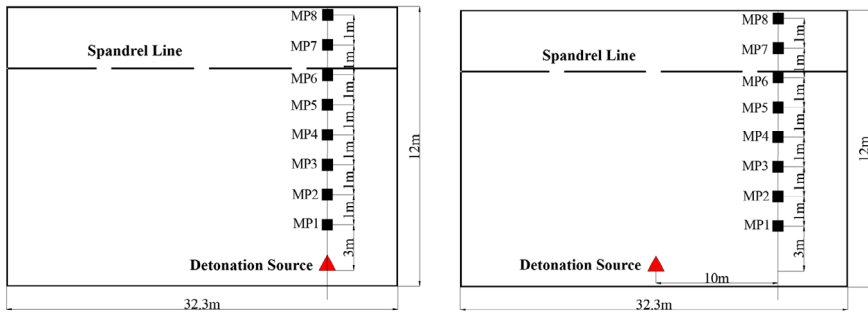
(a) The horizontal distance from the detonation source is 0m

(b) The horizontal distance from the detonation source is 10m
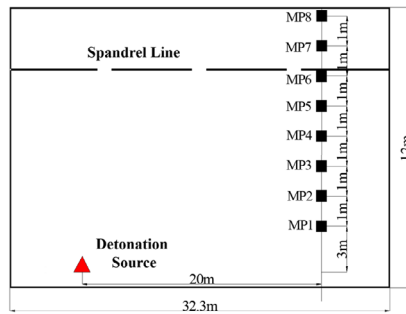
(c) The horizontal distance from the explosion source is 20m

Fig. 3 Layout diagram of blasting vibration measurement points in the test hole

from monitoring is sorted into a graph, which can more intuitively observe the vibration velocity propagation of blasting vibration in three directions along the elevation direction in underground caverns, as shown in Fig. 5.

The test results of blasting vibration velocity obtained from a series of measuring points arranged along the elevation direction in underground caverns are drawn into a curve graph with the horizontal axis X as the elevation and the vertical axis Y as the particle vibration velocity. The following laws can be intuitively found:

① In the test data of the chamber, the horizontal tangential X-direction vibration velocity is the largest, followed by the vertical Z-direction vibration velocity, and the horizontal radial Y-direction vibration velocity is the smallest, that is, $V_X > V_Z > V_Y$. The particle vibration velocity under the influence of blasting vibration is correlated with the constrained condition, and the vibration velocity is inversely proportional to the constrained condition. The greater the constraint, the smaller the vibration velocity generated by the particle.

② The attenuation law of blasting vibration propagation in the elevation direction is different from that in the horizontal direction, and an approximate "platform" curve feature of slow attenuation appears in the middle of the side wall. The accuracy of prediction of this section is low by Sadowski's formula. By conducting the blasting vibration test in the elevation direction in the cave, it can be found that the propagation law of blasting vibration in the middle of the side wall not only fails to meet the Sadowski formula, but also differs from the propagation law of the elevation direction of the open-pit slope. As can be seen from the measured results in Fig. 5 (a) and (b), when the horizontal distance is 0 m, the blasting

Fig. 4 Site layout of underground tunnel indoor test

vibration attenuates rapidly between MP1 and MP3 in the near area before it attenuates in the middle of the side wall in the elevation direction, and the attenuation law is similar to that of the blasting vibration in the horizontal direction. However, from the middle position of the side wall MP4 to the position of MP6, a curve feature of an approximate platform appears, indicating that the elevation amplification effect occurs at this position.

③ It can be seen from Fig. 5 (c) that when the horizontal distance between the measuring point and the explosion source is 10 m, the attenuation law and the trend of blasting vibration in the elevation direction are similar to the elevation propagation law shown in Fig. 5 (b) when the horizontal distance is 0 m. However, due to the increase of the horizontal distance, this location is in the middle area of blasting, and the attenuation trend is slower than that of the horizontal distance of 0 m. However, the local amplification effect appears in the process of blasting vibration propagation in the elevation direction.

④ As can be seen from Fig. 5 (d), when the horizontal distance between the measuring point and the explosion source is 20 m, the attenuation law and the trend of blasting vibration in the elevation direction are different from the elevation propagation law shown in Fig. 5 (b) and (c) when the horizontal distance is 0 m and 10 m. Although there is still local amplification effect in the elevation direction, due to the relatively far horizontal distance of 20 m, the slow attenuation of blasting here is also one of the reasons that the local amplification effect in the elevation direction is more significant, and the blasting vibration velocity value at this location is relatively small, so the impact of blasting vibration is relatively small.

Table 1 Summary of test results of the underground cavern blasting test

| Point number	Q (kg)	D (m)	H (m)	V_X (cm/s)	Master frequency f (Hz)	V_Y (cm/s)	Master frequency f (Hz)	V_Z (cm/s)	Master frequency f (Hz)
MP1	2	0	3	18.12	109.9	11.7	359.9	17.37	420.9
MP2		0	4	12.51	203.8	6.52	203.8	11.41	123.8
MP3		0	5	8.06	57.2	5.16	57.2	8.54	312.2
MP4		0	6	7.53	274.7	4.99	169.2	7.08	95.7
MP5		0	7	6.93	123.8	4.17	137.9	6.12	95.8
MP6		0	8	6.06	31.9	3.99	156.2	5.78	312.5
MP7		0	9	3.99	59.2	3.27	3.5	3.8	142.2
MP8		0	10	2.97	137.9	2.78	59.2	3.01	142.9
MP1	4	0	3	25.72	156.2	15.55	91.9	23.47	156.2
MP2		0	4	17.95	142.2	8.33	142.2	16.1	30.2
MP3		0	5	13.29	403.6	6.08	127.4	11.25	29.2
MP4		0	6	12.83	95.1	5.45	95.4	10.96	142.9
MP5		0	7	11.38	113.2	5.35	83.4	10.78	285.2
MP6		0	8	11.54	33.5	4.74	132.5	10.21	8.5
MP7		0	9	5.28	102.7	3.27	97.4	5.13	7.9
MP8		0	10	4.08	8.5	2.12	42.5	3.99	81.2
MP1	4	10	3	4.55	313	1.6	90.1	3.81	260.4
MP2		10	4	4.03	176	1.39	85.2	2.72	293
MP3		10	5	3.62	313	1.33	88.4	2.32	334.8
MP4		10	6	3.51	156	1.31	156.2	2.44	187.5
MP5		10	7	3.47	99.7	1.19	58.6	2.56	195.3
MP6		10	8	3.27	234	1.09	99.7	2.38	76.8
MP7		10	9	2.74	162	0.81	104.2	1.84	97.7
MP8		10	10	2.46	123	0.56	260.4	1.78	293
MP1	4	20	3	1.67	173.6	1.05	66	1.54	15.7
MP2		20	4	1.55	93.8	1.01	156.2	1.5	82.2
MP3		20	5	1.45	93.8	0.92	75.6	1.37	85.2
MP4		20	6	1.38	114.3	0.881	63.3	1.45	82.2
MP5		20	7	1.39	76.8	0.8	80.8	1.25	76.8
MP6		20	8	1.28	82.2	0.61	66	1.07	79.4
MP7		20	9	1.24	85.2	0.58	73.2	0.94	82.2
MP8		20	10	1.21	3.5	0.45	40.2	0.88	33.3

## 3.3 Calculation formula of blasting vibration

3.3.1 Dimensional analysis

The attenuation law of blasting vibration is closely related to the size of charge, the distance between measuring point and blasting source, and the difference of elevation (Tang and Li 2011). Based on the dimensional homogeneous theorem (Π theorem), the functional
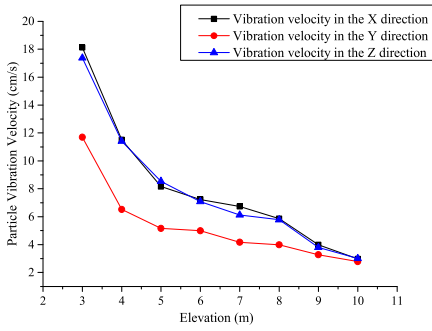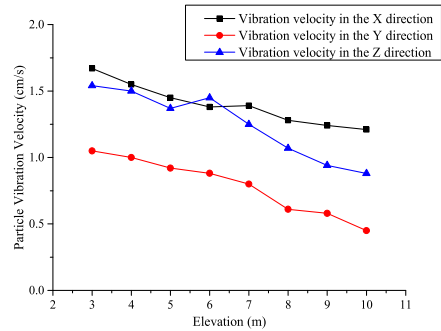
(a) Curves of blasting test results of 2kg charge
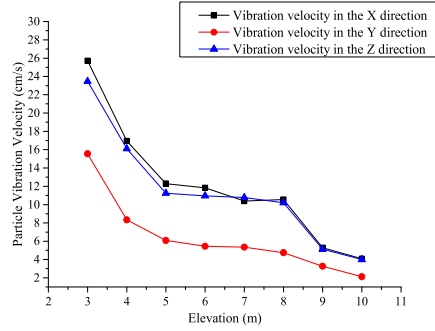
(b) Curves of blasting test results of 4kg charge
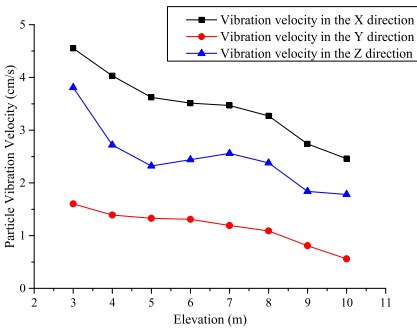
(c) The horizontal distance from the explosion source is 10m

(d) The horizontal distance from the explosion source is 20m

Fig. 5 Curves of blasting test results in the underground cavern

Table 2 Important physical quantities involved in blasting vibration

Variable type	Symbol	Symbolic meaning	Dimension
Dependent variable	V	Particle vibration velocity of rock mass	LT^{-1}
	f	Rock mass particle vibration frequency	T^{-1}
	Q	Explosive mass	M
	r	Detonation distance	L
Argument	H	Elevation difference between measuring point and detonation source	L
	ρ	Rock mass density	ML^{-3}
	c	The propagation speed of a vibrating wave	LT^{-1}
	t	Detonation time	T

equation of vibration velocity V of medium particle is constructed as follows:

$$V = \Phi(Q, \ c, \ \rho, \ r, \ H, \ f, \ t). \tag{12}$$

It can be clearly seen from Table 2 that the physics problem of this research mainly involves 10 physical quantities, that is, n equals 10. According to the dimensional homogeneous theorem, there are three independent dimensional physical quantities, namely Q, r,

and c, which means that they may constitute "n − m = 7" dimensionless parameters, and then the dimensionless equation can be constructed as follows:

$$\Pi = \frac{V}{Q^\alpha r^\beta c^\gamma}. \tag{13}$$

In the above formula, parameters α, β, and γ all represent undetermined coefficients. Based on the dimensional homogeneous theorem, the following equation can be further derived:

$$\dim V = LT^{-1} = (M)^\alpha (L)^\beta \left(LT^{-1}\right)^\gamma. \tag{14}$$

By solving the above formula, it can be obtained that the values of the three undetermined coefficients α, β, and γ are 0, 0, and 1 respectively, and then formula (14) can be further converted into

$$\Pi = \frac{V}{c}. \tag{15}$$

At the same time, the following formula can be solved:

$$\Pi_1 = \frac{f}{Q^{\alpha_1} r^{\beta_1} c^{\gamma_1}}. \tag{16}$$

$\alpha_1 = 0$, $\beta_1 = -1$, $\gamma_1 = 1$. The following formula can be obtained:

$$\Pi_1 = \frac{f}{r^{-1}c}. \tag{17}$$

The same process can be solved:

$$\left.\begin{array}{l} \Pi_2 = \frac{H}{r}, \\ \Pi_3 = \frac{\rho}{Qr^{-3}}, \\ \Pi_4 = \frac{t}{rc^{-1}}. \end{array}\right\} \tag{18}$$

By substituting Eqs. (15), (17)~(18) into functional equation (12), we can get

$$\frac{V}{c} = \Phi\left(\frac{f}{r^{-1}c}, \frac{H}{r}, \frac{\rho}{Qr^{-3}}, \frac{t}{rc^{-1}}\right). \tag{19}$$

Because the product and power of tens of thousands of different dimensionless numbers are still dimensionless numbers (Yang et al. 2018; Tang and Li 2011), then Π_2, Π_3, the new dimensionless number Π_5 can be obtained:

$$\Pi_5 = \Pi_2 \sqrt[3]{\Pi_3} = \left(\frac{H}{r}\right)\left(\frac{\sqrt[3]{\rho}}{\sqrt[3]{Q}/r}\right). \tag{20}$$

For a specific site, ρ and c can be approximated as constants. Therefore, according to (19) and (20), V and $(\frac{H}{r})(\frac{1}{\sqrt[3]{Q}/r})$ can be considered to have a functional relationship. Considering the attenuation relationship between blasting vibration and H/r, the function formula can be expressed as follows:

$$\ln V = \alpha_1 + \beta_1 \ln\left(\frac{\sqrt[3]{Q}}{r}\right) - \left[-\alpha_1' + \beta_1' \ln\left(\frac{H}{r}\right)\right]. \tag{21}$$

If $\ln V_0 = \alpha_1 + \beta_1 \ln(\frac{\sqrt[3]{Q}}{r})$, then

$$\ln V_0 = \alpha_1 + \frac{1}{3}\beta_1 \ln Q - \beta_1 \ln r. \tag{22}$$

In the above formula, parameter $-\beta_1 \ln r$ represents the attenuation relationship between blasting vibration velocity and blast source distance r. Parameter β_1 mainly represents the attenuation coefficient of geological conditions in the blasting area. Parameter $\alpha_1 + \frac{1}{3}\beta_1 \ln Q$ reflects the contribution of geological conditions and the amount of explosive to the particle vibration of the medium. Assuming $\ln k_1 = \alpha_1$, the following equation can be obtained:

$$V_0 = k_1 \left(\frac{\sqrt[3]{Q}}{r}\right)^{\beta_1}. \tag{23}$$

The above formula mainly represents Sadowski's formula in the flat terrain environment. Substitute (23) into (21) to get

$$\ln V = \ln V_0 - \left[-\alpha_1' + \beta_1' \ln\left(\frac{H}{r}\right)\right] = \ln V_0 + \alpha_1' + \beta_1' \ln\left(\frac{H}{r}\right)$$
$$= \ln k_1 \left(\frac{\sqrt[3]{Q}}{r}\right)^{\beta_1} + \alpha_1' + \beta_1' \ln\left(\frac{H}{r}\right). \tag{24}$$

If $\ln k_1 = \alpha_1'$, $\beta_2 = -\beta_1'$, then

$$V = k_1 k_2 \left(\frac{\sqrt[3]{Q}}{r}\right)^{\beta_1} \left(\frac{H}{r}\right)^{\beta_2}. \tag{25}$$

In the above formula, k_1 represents the coefficient of geological conditions under flat terrain; k_2 represents the influence coefficient of complex concave-convex terrain such as slope. β_1 represents the attenuation coefficient of geological conditions in the blasting area; β_2 represents the influence coefficient of elevation difference between the measuring point and the blasting source. Formula (25) derived in this research is no different from other empirical formulas for measuring blasting vibration. It mainly measures the basic physical quantities such as vibration velocity, blast source distance, elevation difference, and ammunition quantity, respectively, and constructs regression equation. From this, basic parameters such as k_1 are further obtained, and the blasting vibration in a form of formula (25) is further derived.

3.3.2 Regression analysis

Since Sadowski's formula does not take the influence of elevation factor into account when predicting particle vibration velocity, the test results obtained by the test are simply analyzed by single-element regression, and the regression value obtained does not reflect the correlation with the height difference of the measured points, so there is a large gap with the measured data, with an average error between 30% and 50%. Therefore, on the premise of considering the elevation factor, the variables related to the elevation are added for binary

Fig. 6 Binary linear regression analysis curve of blasting vibration test data

$$Y=3.8577+1.4405X_1-0.1606X_2$$
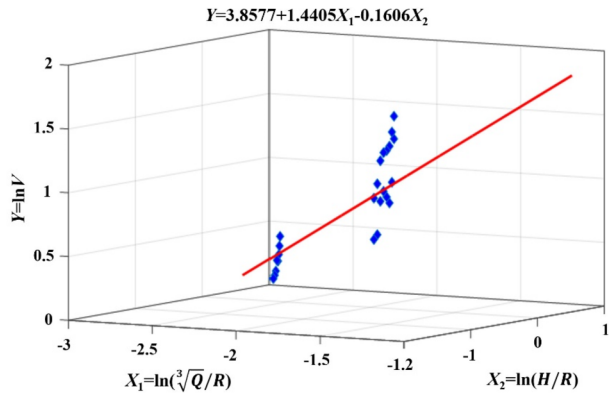
regression analysis, and the logarithms of both sides of equation (25) are respectively taken to obtain

$$\ln V = \ln K' + \alpha \ln\left(\frac{\sqrt[3]{Q}}{R}\right) + \beta \ln\left(\frac{H}{R}\right). \tag{26}$$

If $Y = \ln V$, $C = \ln K'$, $X_1 = \ln(\sqrt[3]{Q}/R)$, $X_2 = \ln(H/R)$, then you can get random variables with X_1, X_2, Y as a random binary equation of dependent variable:

$$Y = C + \alpha X_1 + \beta X_2. \tag{27}$$

Since the research object is the elevation effect of vibration velocity, 24 groups of representative data from field measured data should be selected for binary primary regression analysis. Since the measured data with a horizontal distance of 0 m are substituted into the formula, the regression process did not meet the requirements, so the measured data in the X direction and the Z direction with a horizontal distance of 10 m are selected. As well as the field test data of blasting vibration in the X direction with a horizontal distance of 20 m, the 24 groups of data measured are analyzed by using MATLAB software, as shown in Fig. 6, and the revised Sadowski expression (28) considering the elevation factor is obtained, whose regression coefficient $R = 0.89$, showing good correlation:

$$V = 47.37\left(\frac{\sqrt[3]{Q}}{R}\right)^{1.4405}\left(\frac{H}{R}\right)^{-0.1606}, \quad \text{correlation coefficient } R = 0.89. \tag{28}$$

By considering the dimensionality analysis of the elevation factors, the modified Sadowski formula is obtained by using MATLAB regression fitting software, and the relationship between the particle vibration velocity in the elevation direction, the dose Q, the horizontal distance S, and the elevation H is obtained. As can be seen from equation (28), the influence coefficient of β-elevation difference is -0.1606, less than 0. Therefore, the correction term of blasting vibration velocity in the elevation direction, which only considers elevation factor, will no longer be monotonically inversely proportional to the horizontal distance and directly proportional to charge quantity, and its magnitude is also affected and determined by the ratio of elevation to the horizontal distance. Under local conditions, the local magnification effect under the influence of elevation factors can be reflected by Sadowski's empirical formula.

4 Analysis of numerical results of surrounding rock damage under elevation effect

4.1 Model selection and establishment

(1) Constitutive model

When numerical simulation is used to discuss rock dynamics, the constitutive model of plastic follow-up strengthening is closer to the actual situation and can reflect the mechanical conditions of surrounding rock during detonation relatively accurately and objectively, so the plastic follow-up strengthening model is chosen in this paper (Li and Ma 1992; Tan et al. 2001). The specific expression is as follows (Li et al. 2018):

$$\sigma_y = \left[1 + \left(\frac{\dot{\varepsilon}}{C} \right)^{\frac{1}{p}} \right] (\sigma_0 + \beta E_p \varepsilon_{\text{eff}}^p),\tag{29}$$

$$E_p = \frac{E_0 E_{\text{tan}}}{E_0 - E_{\text{tan}}}.\tag{30}$$

In the above equation, parameter $\dot{\varepsilon}$ represents the strain rate; C and P represent strain rate related parameters in Cowper–Symonds, take $C = 2.5$ s^{-1}, $P = 4$, respectively. In addition, parameter σ_0 represents the initial yield stress of rock; β is the hardening coefficient. When the value is zero, it indicates that the material is plastic follow-up strengthening, and when the value is 1, it indicates that the material is isotropic strengthened. And in between, it is mixed reinforcement. Here, the author chooses the plastic follow-up strengthening to calculate; E_p, E_0, and E_{tan} represent the plastic strengthening modulus, Young's modulus, and tangential modulus, respectively. In the above formula, parameter $\varepsilon_{\text{eff}}^p$ represents the effective plastic strain.
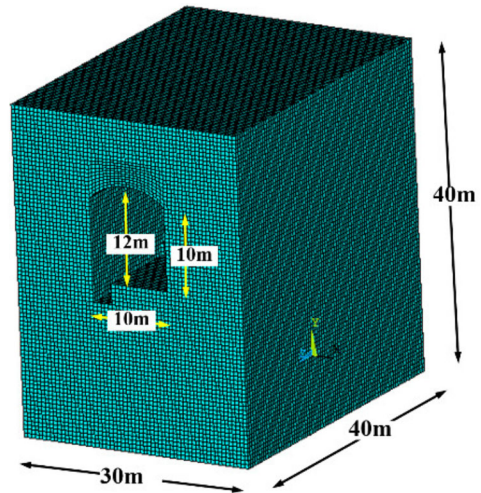
(2) Calculation model

ANSYS/LS-DYNA dynamic finite element software is used to establish the three-dimensional calculation model of the underground cavern in Taohuazui mining area of Sanxin Company (LSTC 2003; Li et al. 2017). The simulated underground cavern is selected in the middle of the whole model, and the foundation size of the cavern is selected according to the actual value of the in-situ test conducted. The height of the straight wall is 10 m. The maximum height of the cavern, which is the distance between the bottom plate and the top arch, is 12 m, and the span is 10 m. In the calculation process, to avoid the influence of boundary conditions on the calculation results, the external dimensions of the model, including height, width, and thickness, are $40 * 30 * 30$ m. The dimensions of the three-dimensional model are shown in Fig. 7. The material mechanical parameters of rock mass are subject to the field measurements in underground caverns, and the main parameters are sorted out as shown in Table 3 according to the geological data obtained from on-site geological exploration.

4.2 Comparative analysis of vibration velocity between numerical calculation and on-site testing results

Before the analysis of numerical calculation results, the field measured data of each measurement point in the in-situ blasting vibration test are compared with the numerical calcu-

Fig. 7 Finite element model of the underground cavern

Table 3 Rock mass physical and mechanical material

$\rho/(kg/m^3)$	E/GPa	μ	σ_t/MPa	σ_c/MPa	E_t/MPa
2600	53.5	0.21	6.0	100.0	8.0

lation results of the corresponding points in the numerical calculation model, so as to verify the reliability of experimental measuring results and numerical calculation results.

According to the in-situ test results of blasting vibration in the underground cavern, the blasting vibration velocity values of three groups of elevation measuring points with horizontal distance of 0 m, 10 m, and 20 m from the blast source are taken as measured data. To further improve the accuracy and reliability of the numerical simulation results, five numerical calculation models of blasting blocks at different positions under the same working conditions are numerically calculated. According to the comparative analysis of vibration velocity data of the experimental measuring points and the simulated measuring points of three groups (as shown in Fig. 8), it is found that the measured data and the calculated results are in high agreement, and the variation trend is basically the same, which can verify the accuracy and reliability of the numerical calculation.

4.3 Analysis of damage calculation results of the underground powerhouse

Under the condition that the original calculation model of an underground cavern and related parameters are completely unchanged, the surrounding rock damage caused by the elevation effect of blasting vibration in the underground cavern is numerically calculated, and the maximum and minimum principal stress nephogram of an excavation model of each layer of the underground cavern is obtained by using the post-processing program, as shown in Fig. 9.

According to Fig. 9, the nephogram analysis of the maximum and minimum principal stress of blasting excavation models in different layers of underground caverns under the blasting load just applied can be found as follows:
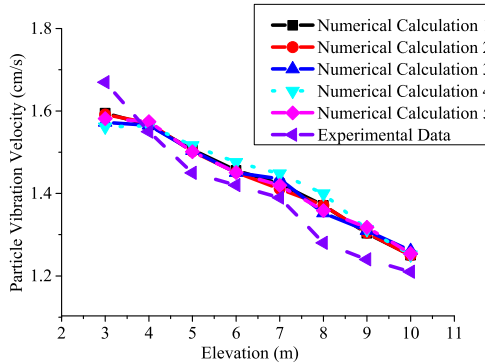
Fig. 8 Contrast analysis diagram between numerical calculation results and experimental data of corresponding measurement points
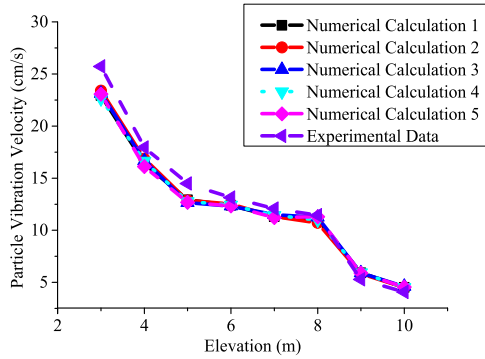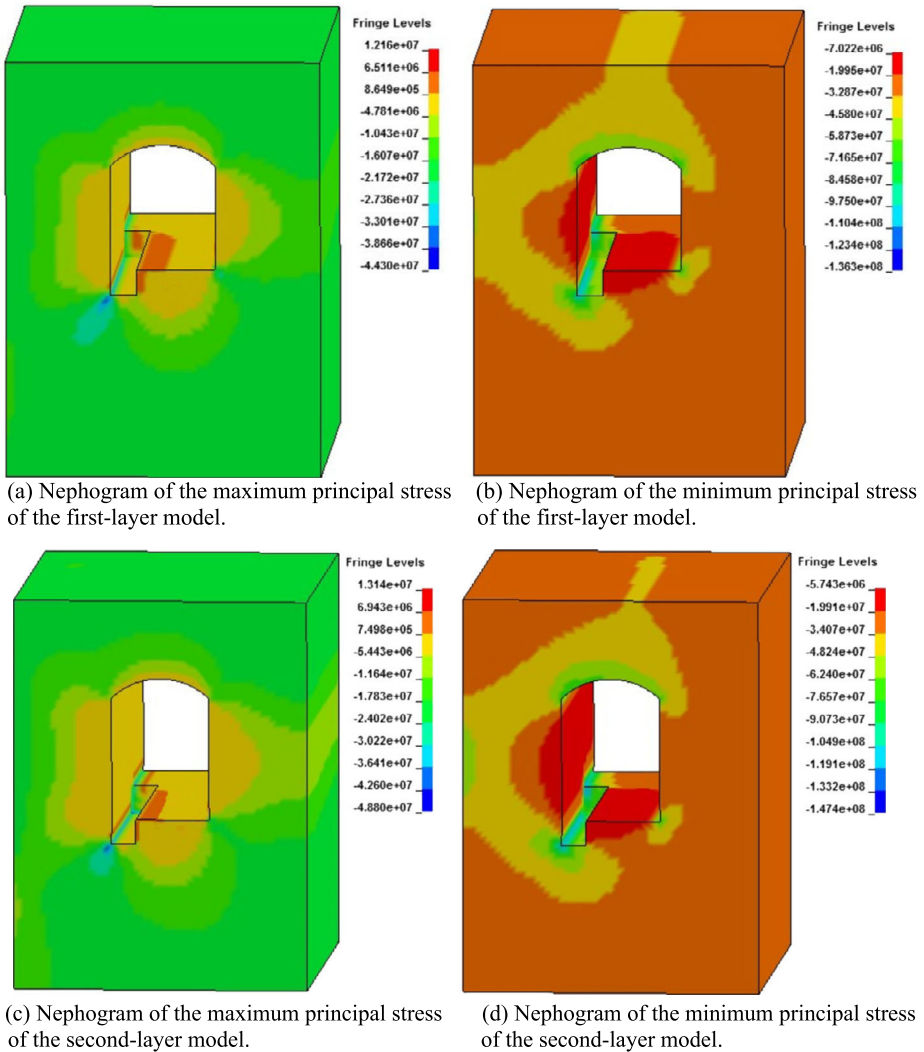

(a) Horizontal distance of 0m
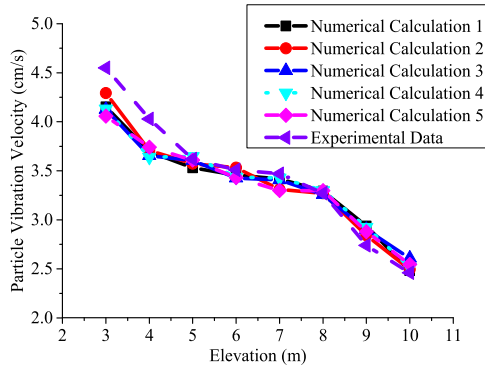
(b) Horizontal distance of 10m

(c) Horizontal distance of 20m

① At the instantaneous moment after blasting load is applied to underground caverns, the maximum principal stress on the surrounding rock of caverns includes tensile stress and compressive stress, in which the tensile stress is positive and the tensile stress is negative. The minimum principal stress of surrounding rock is mainly influenced by compressive stress.

② According to the five maximum principal stress diagrams in Fig. 9 (a), (c), (e), (g), and (i), it can be found that the maximum principal stress in this figure is tensile stress, and all

(a) Nephogram of the maximum principal stress of the first-layer model.

(b) Nephogram of the minimum principal stress of the first-layer model.

(c) Nephogram of the maximum principal stress of the second-layer model.

(d) Nephogram of the minimum principal stress of the second-layer model.

Fig. 9 Principal stress nephogram of excavation model of each layer of underground cavern

of them reach more than 10 MPa, far exceeding the ultimate tensile strength of surrounding rock 4.35 MPa. The corresponding red and orange regions of maximum tensile stress appear. All of them represent the areas where tensile damage occurs. Through comparative analysis of the five Blessings diagram, it can be seen that, with the continuous downward excavation of the cavern and the increase of the cavern height, the area of tensile damage appears to be decreasing on the surface. However, in fact, the observed value of tensile stress shows that with the increase of the cavern height, the maximum tensile stress on the surrounding rock of the cavern increases continuously. When it is increased to a certain extent and exceeds the ultimate tensile strength of rock mass, a new tensile damage zone will appear. In fact, the damage of side wall will increase with the increase of height.
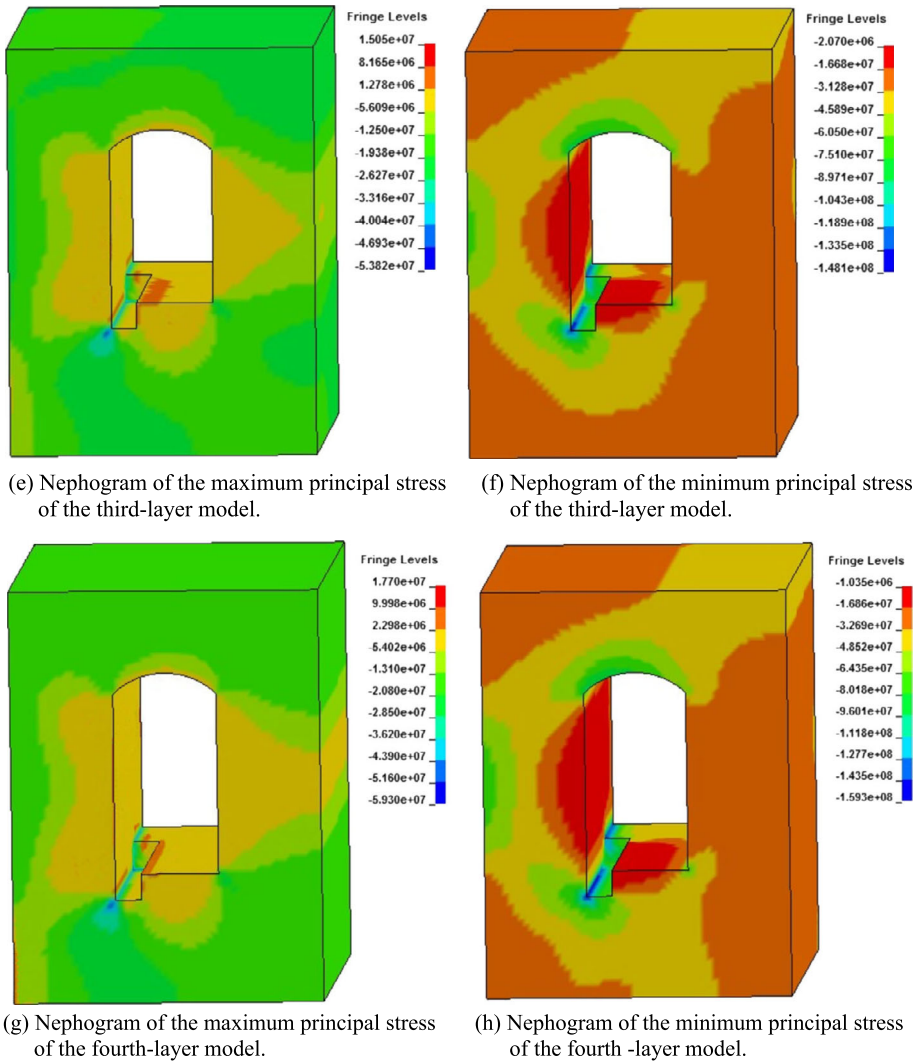
(e) Nephogram of the maximum principal stress of the third-layer model.

(f) Nephogram of the minimum principal stress of the third-layer model.

(g) Nephogram of the maximum principal stress of the fourth-layer model.

(h) Nephogram of the minimum principal stress of the fourth -layer model.

Fig. 9 (*Continued*)

③ According to the five minimum principal stress diagrams in Fig. 9 (b), (d), (f), (h), and (j), it is found that with the downward progress of excavation, the height of the side wall keeps increasing, and the maximum compressive stress on the surrounding rock of the cave keeps increasing. Although the compressive strength of the rock mass is very high, the simulated parameter here is 90 MPa, and the dynamic compressive strength of the rock is also very high. However, in the fifth floor, the maximum compressive stress has reached 180 MPa. With the increase of the height of the side wall, the surrounding rock gradu-allyshows the corresponding compressive stress concentration in the corner, so there will be compressive shear damage. In addition, with the increase of the excavation depth of the cave, the compressive shear damage area of the surrounding rock will also gradually increase.
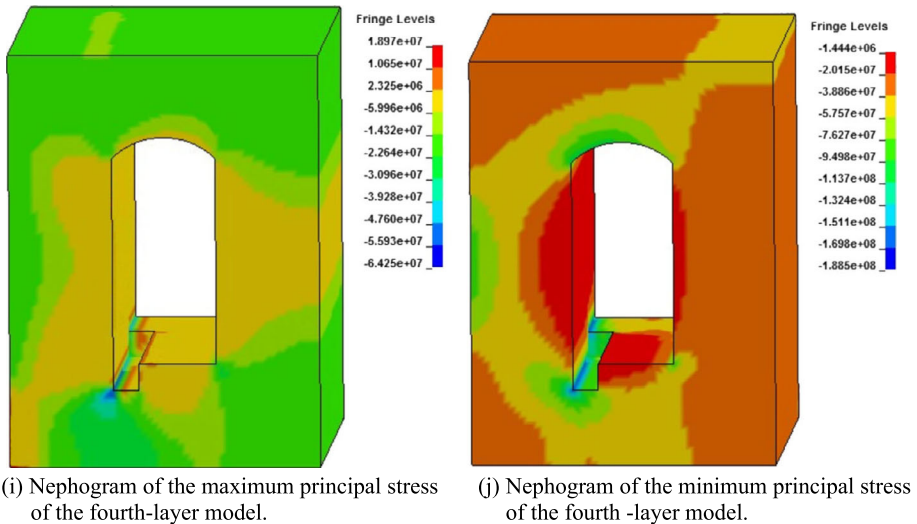
(i) Nephogram of the maximum principal stress of the fourth-layer model.

(j) Nephogram of the minimum principal stress of the fourth -layer model.

Fig. 9 (*Continued*)

4.4 Distribution characteristics of rock mass blasting vibration and damage under elevation effect

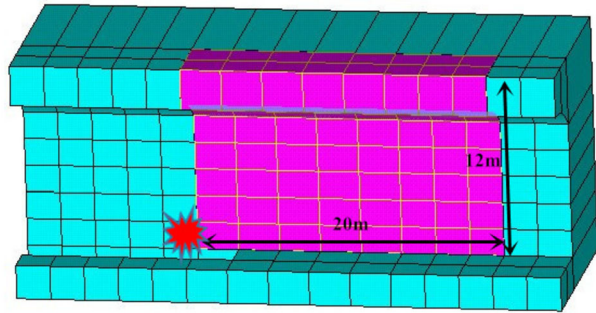### 4.4.1 Particle vibration velocity distribution characteristics of blasting vibration of the underground powerhouse

Taking the explosion source as the origin, a rectangular area with a horizontal distance of 20 m and an elevation of 12 m is selected on the side wall. As the blasting vibration attenuation is very slow and the value is very small beyond 20 m, the distribution characteristics of blasting vibration in the area with a horizontal distance of less than 20 m are mainly studied, as shown in Fig. 10.

The calculated values of particle vibration velocity of all key points in the region selected in Fig. 10 are extracted, and then the particle vibration velocity values of all points in the rectangular region are drawn into the cloud map of distribution characteristics of blasting vibration velocity on the side wall of underground caverns by using MATLAB software, as shown in Fig. 11.

By analyzing the curve characteristics of the cloud image in Fig. 11, the following characteristics of blasting vibration distribution on the side wall of underground cavern can be obtained:

① Blasting vibration in the process of increasing horizontal distance and elevation shows a trend of attenuation on the whole, but there are differences in the attenuation law. The curve in the figure is isoline, and particle vibration velocity of all points on the curve is the same. Therefore, from the perspective of horizontal axis extension direction, the density of the curve is "first dense and then sparse". This shows that the particle vibration velocity attenuates rapidly in the area near the horizontal distance, namely the near-explosion region, and then attenuates more and more slowly with the increase of the horizontal distance, which is consistent with the familiar blasting vibration attenuation law. In the elevation direction, the density change of the curve is not single. The density of the curve first changes from

Fig. 10 Schematic diagram of a blasting vibration distribution area of the underground cavern

Fig. 11 Cloud diagram of vibration velocity distribution characteristics of the side wall of the underground cavern
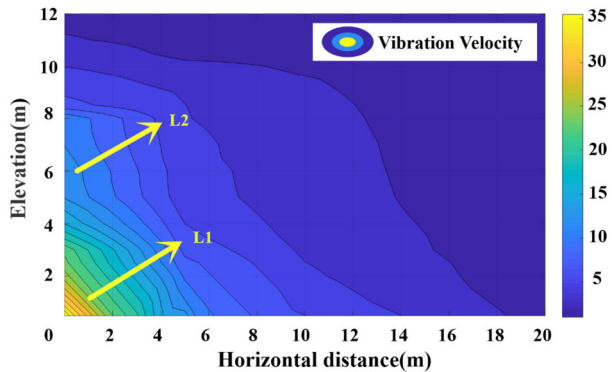
dense to sparse, then becomes dense and sparse again, which indicates that the attenuation coefficient changes in this process. In the range of $0 \sim 5$ m, the attenuation is fast, and then in the range of $5 \sim 8$ m, after 8 m, the attenuation becomes fast and then slow. This process is due to the fact that at 10 m position is the arch foot. At the top of the arch, particle vibration velocity becomes very small and attenuation is slow. From this perspective, it is consistent with the previous numerical calculation results.

② Because the curve in the figure is isoline, the convex from the high-value line to the low-value line in the figure means that the value here is greater than the value around it, indicating that the amplification effect appears at this position. For the position of the two arrows L1 and L2 in the figure, at the position of arrow L1, at the position where the elevation and level are close, the particle vibration velocity increases along the oblique distance and decreases evenly. Compared with the position of L1 and the position of the arrow of L2, the curve with a high value is convex outwards to that with a low value, which indicates that elevation amplification effect occurs at the position with an elevation of about 6–8 m.

③ In the region with an elevation of 5–8 m, there is a certain convex phenomenon in the horizontal direction, namely the amplification effect. However, because the blasting vibration value is very small and attenuation is slow at the part with a long horizontal distance, the elevation amplification effect is not too representative at this time.

4.4.2 Distribution characteristics of blasting damage

The vibration velocity of all the key points in the underground powerhouse in Fig. 11 is converted into the corresponding damage depth of surrounding rock by using the calculation

Fig. 12 Cloud diagram of blasting damage distribution characteristics on the side wall of the underground cavern
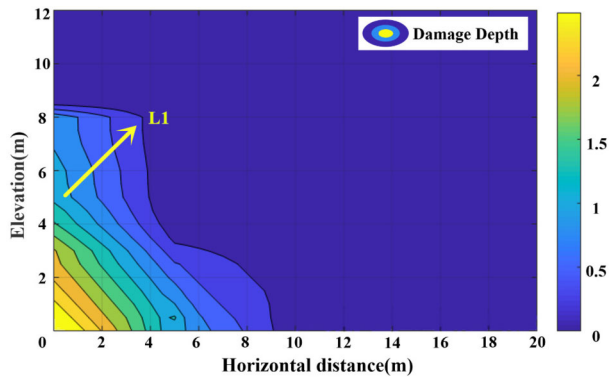
formula, and the cloud map of blasting damage distribution characteristics of the side wall of the underground caverns is drawn by using MATLAB software, as shown in Fig. 12. Therefore, after the particle vibration velocity distribution characteristics are obtained under certain conditions, the corresponding blasting damage distribution characteristics can be obtained.

By studying and analyzing the blasting damage distribution characteristics of underground caverns in Fig. 12, it can be found that:

① The large area of dark blue represents the area where the surrounding rock damage is 0. This part is because in the process of the gradual increase of horizontal distance and elevation, the particle vibration velocity of blasting vibration is small, which does not reach the condition of causing the surrounding rock damage. Therefore, in practical engineering, it is very meaningful to control the damage of surrounding rock by controlling the particle vibration velocity of blasting vibration. There is also a theoretical basis.

② In the area pointed by the arrow L1, the damage of surrounding rock also appears the same amplification as its corresponding particle vibration velocity, indicating that under the influence of the elevation effect of blasting vibration, the blasting damage also has a certain amplification effect in the local position in the elevation direction. Therefore, blasting vibration should be controlled well in the excavation process of an underground cavern, so as to effectively control the damage caused by blasting vibration.

5 Conclusion

According to the blasting damage mechanical characteristics of rock mass, the dynamic finite element software is used to calculate the blasting vibration damage of an underground cavern model under the elevation effect by using the dynamic strengthening constitutive model. The relationship between blasting vibration and surrounding rock damage is studied by in-situ testing in an underground cavern of a mine. The connection between the blasting vibration distribution characteristics under elevation effect and the surrounding rock damage distribution characteristics under elevation effect is established. The main conclusions are as follows:

(1) The mechanical model analysis of the high side wall of an underground cavern is established based on the characteristics of simple supported beams. The dimensional analysis method is adopted to carry out regression analysis on the field data of blasting vibration of underground cavern, and the calculation formula of vibration propagation law of underground cavern blasting under the elevation effect is obtained.

(2) Through numerical calculation, the distribution characteristics of blasting vibration under elevation effect and surrounding rock damage distribution characteristics under elevation effect are established. Through comparative analysis of the damage degree of side walls with different heights, it is found that the maximum tensile stress increases with the increase of the height of the cavern, and a new tensile damage area appears. At the same time, with the increase of excavation depth, the compressive shear damage area of surrounding rock increases gradually.

(3) The particle vibration velocity values of all key nodes in a certain area are extracted, and combined with the established functional relationship between blasting vibration and surrounding rock damage, the surrounding rock damage depth under different particle vibration velocity is calculated, which is drawn into the blasting damage distribution cloud diagram under elevation effect, and the distribution characteristics of local amplification effect of surrounding rock damage under elevation are obtained.

(4) The mode of vibration is often related to the vibration frequency. Due to many uncertain factors affecting vibration frequency, the variation range of frequency value fluctuates greatly. In future research, it is necessary to further analyze and research the influence of vibration frequency on the distribution law of blasting vibration.

(5) The side wall of an underground cavern is often supported by sprayed concrete. The mechanical parameters of sprayed concrete and surrounding rock are different. In future research, it is necessary to consider the influence of different material properties on blasting vibration.

Declarations

Competing interests The authors declare no competing interests.

References

Cai, M., Kaiser, P.K., Tasaka, Y., et al.: Generalized crack initiation and crack damage stress thresholds of brittle rock masses near underground excavations. Int. J. Rock Mech. Min. Sci. **41**(5), 833–847 (2004)

Grady, D.E., Kipp, M.E.: Continuum modelling of explosive fracture in oil shale. Int. J. Rock Mech. Min. Sci. Geomech. Abstr. **17**(3), 147–157 (1980)

Huang, J., Li, X., Luo, Y., Liu, T., Dong, Q., Xu, K.: Numerical simulation of influence of filled joint on the crack formed by notch hole blast. Eur. J. Environ. Civ. Eng. **24**(4), 423–439 (2020). https://doi.org/10.1080/19648189.2017.1392366

Kuszmaul, J.S.: A new constitutive model for fragmentation of rock under dynamic loading. Oil Shales and Tar Sands (1987)

Li, Y., Ma, S.: Explosion Mechanics. Science Press, Beijing (1992)

Li, X., Wang, S., Gao, H.: Analysis of influencing factors of blasting vibration frequency. J. Liaoning Tech. Univ. **2**, 204–206 (2006)

Li, X., Huang, J., Luo, Y., Dong, Q., Li, Y., Wan, Y., Liu, T.: Numerical simulation of blast vibration and crack forming effect of rock-anchored beam excavation in deep underground caverns. Shock Vib. **2017**, 1–13 (2017). https://doi.org/10.1155/2017/1812080

Li, X., Lv, J., Luo, Y., Liu, T.: Mechanism study on elevation effect of blast wave propagation in high side wall of deep underground powerhouse. Shock Vib. **2018**, 4951948 (2018). https://doi.org/10.1155/2018/4951948

Liu, R.S.: The analysis of slippage and coming away between the subway structure and the soil subjected to strong ground motions. Earthq. Eng. Eng. Vib. **24**(6), 136–141 (2004). https://doi.org/10.3969/j.issn.1000-1301.2004.06.024

Liu, J.B., Liu, X.Q., Du, X.L.: Prospects for the development in theoretical analysis and experimental study of seismic response of underground structures. Earthq. Eng. Eng. Vib. **27**(6), 38–44 (2007). https://doi.org/10.13197/j.eeev.2007.06.037

LSTC: LS-DYNA keyword user's manual. Livermore Software Technology Corporation, California (2003)

Pei, X., Zhang, L., Ren, Z.: Time History Analysis of Seismic Response of Tall Building Structures. Intellectual Property Publishing House, Beijing (2006)

Ramulu, M., Chakraborty, A.K., Sitharam, T.G.: Damage assessment of basaltic rock mass due to repeated blasting in a railway tunnelling project-a case study. Tunn. Undergr. Space Technol. **24**(2), 208–221 (2009). https://doi.org/10.1016/j.tust.2008.08.002

Shi, C., Bi, W.: Discussion on failure criterion of blasting earthquake. Rock Soil Mech. Ser. **1**, 115–118 (2004)

Song, G., Chen, S., Shi, X., et al.: Study on blasting vibration monitoring and evaluation method of open-pit mine slope. Non-Ferr. Met. **4**, 24–27 (2000)

Tan, H., Sun, J., Qi, S.: Study on vibration attenuation law of dynamic rammer. Geotech. Investig. Surv. **5**, 11–14 (2001)

Tang, H., Li, H.: Research on blasting vibration formula reflecting elevation amplification effect. Rock Soil Mech. **32**(3), 820–824 (2011)

Tang, C., Yu, Y., Wang, J.: A preliminary study on the safety criterion of blasting ground vibration. Non-Ferr. Met. **1**, 1–4 (2001)

Technical specification for excavation engineering of rock foundation of hydraulic buildings. (DL/T 5389-2007). National Development and Reform Commission, PRC, Beijing, China (2007)

Terzaghi, K.: Evaluation of coefficients of subgrade reaction. Geotechnique **5**(4), 197–326 (1955). https://doi.org/10.1680/geot.1955.5.4.297

Thorne, B.J., Hommert, P.J., Brown, B.: Experimental and computational investigation of the fundamental mechanisms of cratering. Inorganic Organic Physical and Analytical Chemistry (1990)

Tylor, L.M., Chen, E.P., Kuszmanl, J.S.: Microcrack-induced damage accumulation in brittle rock under dynamic loading. Comput. Methods Appl. Mech. Eng. **55**(3), 301–320 (1986)

Wu, D., Ye, X.: Comprehensive study on safety vibration velocity of engineering blasting. Chin. J. Rock Mech. Eng. **3**, 67–74 (2004)

Xu, H., Zhang, J., Yang, H., et al.: Discussion on calculation formula of drilling and blasting vibration velocity and its simplification. J. Tongji Univ. Nat. Sci. **35**(7), 899–903, 914 (2007)

Yang, R., Bawden, W.F., Katsabanis, P.D.: A new constitutive model for blast damage. Int. J. Rock Mech. Min. Sci. Geomech. Abstr. **33**(3), 245–254 (1996)

Yang, R., Ding, C., Yang, L., Chen, C.: Model experiment on dynamic behavior of jointed rock mass under blasting at high-stress conditions. Tunn. Undergr. Space Technol. **74**, 145–152 (2018). https://doi.org/10.1016/j.tust.2018.01.017

Yang, J., Jiang, Q., Zhang, B., Zhao, J.: Dynamic stress adjustment and rock damage during blasting excavation in a deep-buried circular tunnel. Tunn. Undergr. Space Technol. **71**, 591–604 (2018). https://doi.org/10.1016/j.tust.2017.10.010

Zhang, Y., Zhu, Z., Xu, R., Huang, Z.: Effect of seismic frequency spectra on surrounding rock damage evolution of large underground caverns. Adv. Mater. Sci. Eng. **2018**, 1–13 (2018). https://doi.org/10.1155/2018/3265460

Zhao, Z., Zhang, Y., Bao, H.: Tunnel blasting simulations by the discontinuous deformation analysis. Int. J. Comput. Methods **8**(2), 277–292 (2011). https://doi.org/10.1142/S0219876211002599

Zheng, Y., Yang, L., Li, W., et al.: Seismic Resistance of Underground Structure. Tongji University Press, Shanghai (2005)

Zhou, T., Yang, X., Weng, J.: Experimental study on blasting seismic elevation effect. Mine Constr. Technol. Ser. **1**, 32–36 (1997)

Zhou, J., Lu, W., Zhang, L., et al.: Study on attenuation law of vibration frequency during blasting seismic wave propagation. Chin. J. Rock Mech. Eng. **11**, 2171–2178 (2011)

Zhu, C., Liu, H., Mei, J.: The selection of seismic wave parameter propagation rule formula along edge slope. Blasting **2**, 30–31 (1988)

Publisher's Note Springer Nature remains neutral with regard to jurisdictional claims in published maps and institutional affiliations.